The Plant Cell, Vol. 19: 847–861, March 2007, www.plantcell.org © 2007 American Society of Plant Biologists

Rice UDP-Glucose Pyrophosphorylase1 Is Essential for Pollen Callose Deposition and Its Cosuppression Results in a New Type of Thermosensitive Genic Male Sterility [W][OA]

Rongzhi Chen, Xiao Zhao, Zhe Shao, Zhe Wei, Yuanyuan Wang, Lili Zhu, Jie Zhao, Mengxiang Sun, Ruifeng He, and Guangcun He[1]

Key Laboratory of Ministry of Education for Plant Developmental Biology, College of Life Sciences, Wuhan University, Wuhan 430072, China

UDP-glucose pyrophosphorylase (UGPase) catalyzes the reversible production of glucose-1-phosphate and UTP to UDP-glucose and pyrophosphate. The rice (*Oryza sativa*) genome contains two homologous UGPase genes, *Ugp1* and *Ugp2*. We report a functional characterization of rice *Ugp1*, which is expressed throughout the plant, with highest expression in florets, especially in pollen during anther development. *Ugp1* silencing by RNA interference or cosuppression results in male sterility. Expressing a double-stranded RNA interference construct in *Ugp1-RI* plants resulted in complete suppression of both *Ugp1* and *Ugp2*, together with various pleiotropic developmental abnormalities, suggesting that UGPase plays critical roles in plant growth and development. More importantly, *Ugp1*-cosuppressing plants contained unprocessed intron-containing primary transcripts derived from transcription of the overexpression construct. These aberrant transcripts undergo temperature-sensitive splicing in florets, leading to a novel thermosensitive genic male sterility. Pollen mother cells (PMCs) of *Ugp1*-silenced plants appeared normal before meiosis, but during meiosis, normal callose deposition was disrupted. Consequently, the PMCs began to degenerate at the early meiosis stage, eventually resulting in complete pollen collapse. In addition, the degeneration of the tapetum and middle layer was inhibited. These results demonstrate that rice *Ugp1* is required for callose deposition during PMC meiosis and bridges the apoplastic unloading pathway and pollen development.

INTRODUCTION

UDP-glucose pyrophosphorylase (UGPase) is found in all prokaryotic and eukaryotic organisms. It is a key enzyme in carbohydrate metabolism that catalyzes the reversible production of glucose-1-phosphate and UTP to UDP-glucose and pyrophosphate, depending on the metabolic status of the tissue. In photosynthetic source tissues, UGPase is coupled with sucrose phosphate synthase; it converts glucose-1-phosphate to UDP-glucose and is primarily involved in the synthesis of sucrose, the major sugar for photoassimilate export (reviewed in Kleczkowski et al., 2004). In nonphotosynthetic sink tissues, which to some extent depend on imported carbon resources, UGPase is linked to sucrose degradation pathways by converting UDP-glucose produced by sucrose synthase (SuSy) to glucose-1-phosphate for the demand of metabolic processes (Winter and Huber, 2000). In the cytoplasm of cereal seed endosperm, UGPase may also be coupled with cytosolic ADP-glucose pyrophosphorylase, resulting in a direct conversion of UDP-glucose to ADP-glucose for starch synthesis (reviewed in Kleczkowski, 1994).

In addition to its involvement in sucrose and starch metabolism, UGPase also takes part in cell wall biosynthesis. The substrate/product of UGPase, UDP-glucose, acts as a precursor for the synthesis of the carbohydrate moiety of glycolipids, glycoproteins, and cell wall components, including callose, pectin, and cellulose (reviewed in Kleczkowski, 1994; Amor et al., 1995; Gibeaut, 2000; Dong, 2004). UGPase mutant strains of *Dictyostelium* failed to complete the developmental cycle due to insufficient UDP-glucose levels for cellulose formation (Dimond et al., 1976). When the *UgpB* gene is disrupted in *Dictyostelium discoideum*, cells undergo aberrant differentiation and development with decreased spore viability and glycogen levels (Bishop et al., 2002). Also, *Ugp* is involved in cellulose biosynthesis in *Acetobacter xylinum*, as confirmed by its complementation of cellulose-negative mutants (Valla et al., 1989). A 10-fold–reduced UGPase activity in the yeast mutant resulted in a slight increase in the calcofluor sensitivity and a decrease in the cell-wall β-glucan content (Daran et al., 1995). Point mutations in the *UGP* gene lead to cellular UDP-glucose deficiency and decreased glycogen levels (Flores-Diaz et al., 1997).

In plants, *Ugp* genes are expressed in all tissues, including roots, tubers, leaves, stems, and young seeds (Zrenner et al., 1993; Abe et al., 2002). Pi deficiency, light exposure, and sucrose feeding could upregulate its expression, and upregulation of *Ugp* by sucrose is mediated via a hexokinase-independent and

[1] To whom correspondence should be addressed. E-mail gche@whu.edu.cn; fax 86-27-68752327.

The author responsible for distribution of materials integral to the findings presented in this article in accordance with the policy described in the Instructions for Authors (www.plantcell.org) is: Guangcun He (gche@whu.edu.cn).

[W] Online version contains Web-only data.

[OA] Open Access articles can be viewed online without a subscription.

www.plantcell.org/cgi/doi/10.1105/tpc.106.044123

abscisic acid–insensitive pathway that involves an okadaic acid–responsive protein phosphatase (Ciereszko et al., 2001a, 2001b; Kleczkowski et al., 2004). Many *Ugp* genes have been cloned from various species of plants, including potato (*Solanum tuberosum*) (Katsube et al., 1990), barley (*Hordeum vulgare*) (Eimert et al., 1996), and rice (*Oryza sativa*) (Abe et al., 2002). Earlier studies concerning the biological function of plant *Ugp* genes focused on whether it represents a rate-limiting step in carbohydrate metabolism. In stored potato tubers, when UGPase activity was decreased by 30 to 50% by antisense suppression, significant reductions in sugar content were observed (Spychalla et al., 1994; Borovkov et al., 1996). In *Arabidopsis thaliana*, a decrease of 30% in UGPase activity led to a large decrease in carbohydrate content in the antisense plants, but without any detectable changes in plant growth parameters (Johansson, 2003).

The rice genome contains two homologous UGPase genes, *Ugp1* on chromosome 9 (Abe et al., 2002) and *Ugp2* on chromosome 2 (Mu, 2002). The rice *Ugp1* gene on chromosome 9 was first cloned from immature endosperm. Its mRNA level was high at 10 to 15 d after flowering and then slightly decreased until up to 35 d after flowering (Abe et al., 2002). Remarkably, promoter reporter analysis has suggested that the rice *Ugp2* gene on chromosome 2 is expressed only in binucleate pollen (Mu, 2002). Here, we report a detailed functional characterization of rice *Ugp1. Ugp1* is expressed throughout the rice plant, with highest expression in florets, especially in pollen cells during anther and pollen development. Silencing of *Ugp1* by RNA interference (RNAi) or cosuppression affects callose deposition during pollen wall development and leads to the degeneration of the pollen mother cell (PMC) at the early meiosis stage, resulting in male sterility in rice. These results demonstrate that *Ugp1* is essential for PMC meiosis and microspore development in rice. Moreover, *Ugp1*-cosuppressing plants contained unprocessed intron-containing primary transcripts derived from the transcription of the overexpression construct. These aberrant transcripts undergo temperature-sensitive splicing in florets, resulting in a new type of thermosensitive genic male sterility.

RESULTS

Ugp1 Transcript Is Abundant in Florets

The rice genome contains two UGPase genes: *Ugp1* on chromosome 9 (Abe et al., 2002) and *Ugp2* on chromosome 2 (Mu, 2002). They share 81 and 88% sequence identity at the nucleotide sequence and the amino acid levels, respectively. We have previously isolated the rice *Ugp1* gene (Chen et al., 2007). To understand the role of the gene in rice plant development, we first examined its expression in different rice organs by RNA gel blot analysis. The expression pattern is shown in Figure 1A. *Ugp1* was expressed in various organs, including roots, seedling stems, mature stems, seedling leaves, and mature leaves. However, *Ugp1* transcripts were most abundant in pooled florets at various stages before flowering (Figure 1A). A duplicate RNA membrane was hybridized with *Ugp2* probes under the same high stringency conditions as those used to hybridize *Ugp1*, and no visible *Ugp2* signal was detected (data not shown), indicating that the

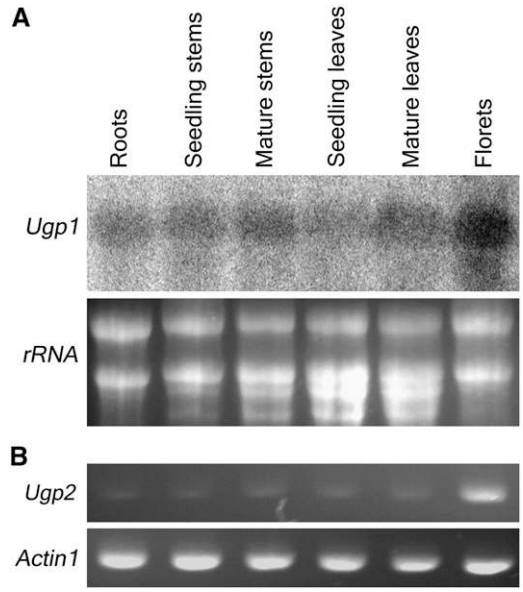

Figure 1. Expression Patterns of *Ugp1* and *Ugp2* in Wild-Type Hejiang 19 Rice Plants.

(A) RNA gel blot analysis of *Ugp1* transcript levels in wild-type Hejiang 19 rice plants. Total RNA (20 μg) extracted from wild-type tissues, including roots, seedling stems, mature stems, seedling leaves, mature leaves, and pooled florets at various stages before flowering was probed with full-length *Ugp1* cDNA. An ethidium bromide stain of the gel is shown to confirm equal RNA loading.

(B) RT-PCR analysis of *Ugp2* expression in wild-type Hejiang 19 rice plants. The amplification of the rice *Actin1* gene was used as a control to show that approximately equal amounts of total RNA had been used in the RT-PCR analysis.

Ugp mRNA bands shown in Figure 1A consist solely of *Ugp1* transcripts and that *Ugp2* is expressed at extremely low levels. We therefore performed a more sensitive method, semiquantitative RT-PCR, to estimate the level of *Ugp2* transcript. Low but detectable levels of *Ugp2* transcript were found in roots, seedling stems, mature stems, seedling leaves, and mature leaves (Figure 1B). *Ugp2* transcripts were also present at higher levels in pooled florets at various stages before flowering (Figure 1B). Together, these data indicate that both *Ugp1* and *Ugp2* are ubiquitously expressed throughout rice development and that *Ugp1* is expressed at much higher levels than *Ugp2*. The presence of greater amounts of *Ugp1* transcripts in florets before flowering strongly suggests that it plays a special role in rice flower development.

Identification of *Ugp1*-Overexpressing, *Ugp1*-Cosuppressing, and *Ugp1*-RNAi Transgenic Rice Plants

To elucidate the role of *Ugp1* in rice growth and development, we constitutively increased and suppressed the expression of the *Ugp1* gene in transgenic rice. The overexpression construct (*Ugp1-OX*), antisense construct (*Ugp1-AS*), and double-stranded

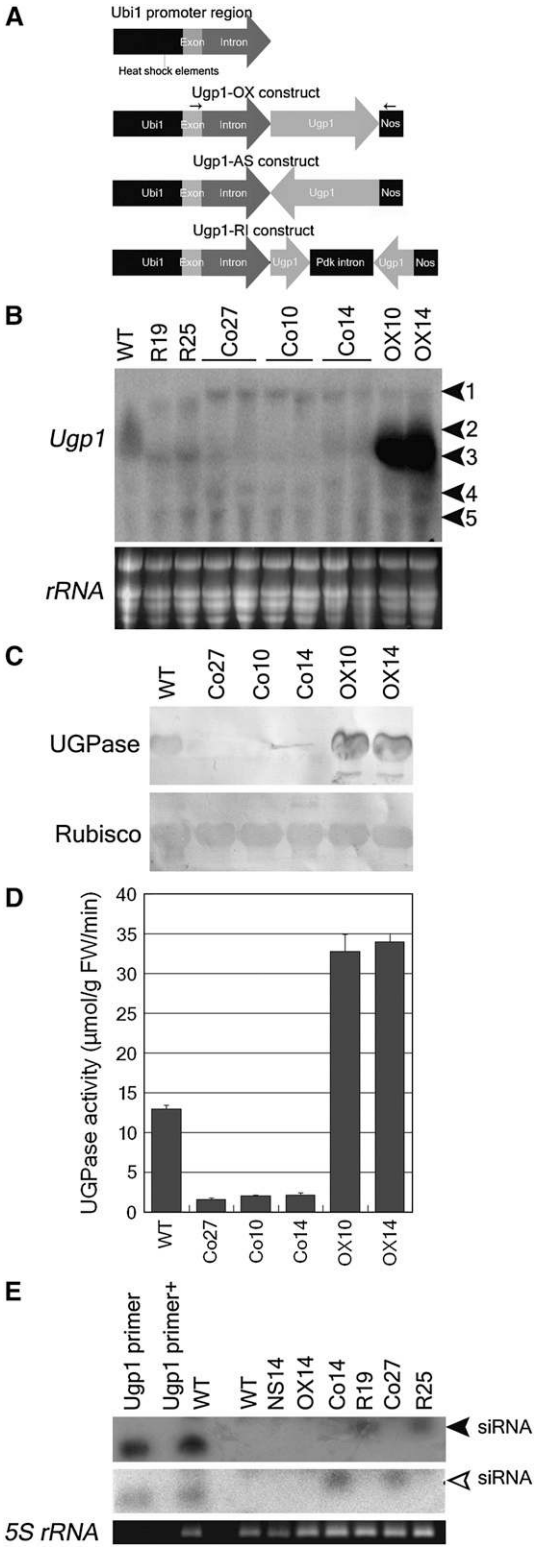

Figure 2. *Ugp1* Expression Patterns in Transgenic Rice Plants.

(A) Structures of constructs for rice transformation. The promoter of the maize ubiquitin 1 gene of ~2 kb comprises, in the 5′ to 3′ direction, the following: a promoter with a transcription start site (+1); two overlapping heat shock elements located at positions −214 and −204 from the transcription start site; an 83-bp leader sequence adjacent to the transcription start site (exon); an intron of ~1 kb; and a translation start site. The overexpression construct (*Ugp1-OX*), antisense construct (*Ugp1-AS*), and dsRNAi construct (*Ugp1-RI*) of *Ugp1* were developed under the control of the *Ubi1* promoter and nopaline synthase (Nos) terminator cassette. Arrows represent the primers used to generate the RT-PCR products shown in Figure 7D.

(B) RNA gel blot analysis of *Ugp1* transcript levels in transgenic rice. Total RNA extracted from rice plants at the heading stage was probed with full-length *Ugp1* cDNA. Arrowheads indicate (1) the unprocessed longer-than-full-length transcript and (2) endogenous *Ugp1* mRNA; (3) to (5) indicate the silencing-related RNA degradation intermediates. Loading of equal amounts of RNA was confirmed by ethidium bromide staining.

(C) Protein gel blot analysis of UGPase protein from transgenic plants using an antibody against rice UGPase. Equal loading of proteins in each lane was confirmed by probing a duplicate blot with an anti-ribulose-1, 5-bisphosphate carboxylase/oxygenase (Rubisco) antibody.

(D) UGPase activities in transgenic plants. UGPase activities are shown as means ± SE ($n = 3$).

(E) siRNA analysis in transgenic plants. Seventy-five nanograms of *Ugp1* primers (18 and 21 nucleotides) were intermixed or mixed with wild-type RNA and served as size standard and hybridization controls. Closed arrowhead indicates the siRNA probed by the *Ugp1* cDNA fragment between +333 and +852 (related to the ATG at +1 bp), and the open arrowhead indicates the siRNA by the 3′-end of the *Ugp1* coding region. 5S rRNA was used as the loading control.

Co10, Co14, and Co27, cosuppressing plants of lines 10, 14, and 27, respectively; OX10 and OX14, overexpressing plants of lines 10 and 14, respectively; NS14, null segregant plant of line 14; R19 and R25, RNAi plants of lines 19 and 25, respectively.

RNA interference (dsRNAi) construct (*Ugp1-RI*) of *Ugp1* were developed under the control of the maize (*Zea mays*) ubiquitin 1 (*Ubi1*) promoter (Christensen et al., 1992; Christensen and Quail, 1996) (Figure 2A). Transgenic plants were generated by introducing the constructs into the japonica rice variety Hejiang 19 by *Agrobacterium tumefaciens*–mediated transformation (Hiei et al., 1994). Forty independent *Ugp1-OX* plants (T0 generation), 24 independent antisense *Ugp1-AS* T0 plants, and 20 independent *Ugp1-RI* T0 plants were generated, each containing one to several copies of the transgene, as confirmed by DNA gel blot analysis (data not shown).

Ugp1-OX T0 plants with a single T-DNA insertion were selected for further characterization. T1 lines were germinated and transplanted in the field at Wuhan University on April 28 and May 27, 2004. T1 plants carrying the *Ugp1-OX* construct were identified by PCR amplification of the transgene. Expression of *Ugp1* was examined by RNA gel blot analysis of total RNA extracted from leaves of transgenic plants (Figure 2B). According to the abundance of *Ugp1* transcripts in transgenic plants, the PCR-positive transgenic T1 plants of the *Ugp1-OX* lines segregated into two subpopulations. In one subpopulation, referred to as overexpressing plants, *Ugp1* mRNA strongly accumulated (Figure 2B, OX10 and OX14). In the other subpopulation, endogenous *Ugp1* expression was completely suppressed; no signal was detected in the regions corresponding to endogenous *Ugp1* mRNA (Figure 2B, Co27, Co10, and Co14), suggesting that it was

cosuppressed (Napoli et al., 1990; van der Krol et al., 1990). Thus, this subpopulation is referred to as cosuppressing plants. Besides low molecular weight and silencing-related RNA degradation intermediates, longer-than-full-length *Ugp1* mRNAs, which contained the unspliced intron in the 5′-untranslated region of the *Ubi1* promoter, were also present in the cosuppressing plants (Figure 7A).

We also performed protein gel blot analysis to investigate UGPase protein levels in the transgenic plants (Figure 2C). In accordance with the results of the RNA gel blot analysis, very high levels of UGPase protein were detected in the overexpressing plants, whereas UGPase signals in samples from the cosuppressing plants were very weak or undetectable. The UGPase activity correlated well with the amounts of UGPase protein (Figure 2D). The overexpressing plants had almost 260% wild-type UGPase activities, while the cosuppressing plants had only 11% wild-type activities.

RNA gel blot analysis showed that endogenous *Ugp1* mRNA expression was not affected in PCR-positive transgene segregants of the *Ugp1-AS* population (data not shown). These plants exhibited no signs of abnormal growth and development; therefore, they were not studied further.

Ugp1-RI T0 plants were first analyzed by UGPase activity assays. Fourteen out of 20 *Ugp1-RI* T0 plants showed substantial reductions in leaf UGPase activity, ranging from 5.9 to 27.0% of that in wild-type Hejiang 19 control plants (see Supplemental Figure 1 online). Of these, R19 and R25 lines were selected for further molecular analysis. RNA gel blot analysis showed that endogenous *Ugp1* mRNAs in R19 and R25 lines were completely suppressed, as in cosuppressing plants, since no signal was detected in the regions corresponding to endogenous *Ugp1* mRNA (Figure 2B). These results indicate that *Ugp1* was suppressed in these *Ugp1-RI* plants by RNAi (Wesley et al., 2001; Baulcombe, 2004).

To further confirm the silencing of *Ugp1* in *Ugp1-RI* and cosuppressing plants, we examined them for the presence of small interfering RNAs (siRNAs), the hallmark of RNAi and cosuppression (Hamilton and Baulcombe, 1999; Baulcombe, 2004). As shown in Figure 2E, *Ugp1*-derived siRNAs were detected in the *Ugp1-RI* plants and cosuppressing plants, but not in any wild-type, null segregant, or overexpressing plants examined. In the *Ugp1-RI* lines, the only siRNAs detected corresponded to the region (333 to 852) designed to produce the inverted repeat hairpin RNA, while in cosuppressing plants, the detected siRNAs corresponded to the 3′-end of the *Ugp1* coding region. Both the *Ugp1-RI* and cosuppressing plants showed no presence of siRNAs corresponding to the 5′-end of the *Ugp1* coding region (data not shown). Taken together, these results strongly suggest that *Ugp1* was silenced in both the *Ugp1-RI* and cosuppressing plants.

Silencing of *Ugp1* by RNAi or Cosuppression Results in a Male-Sterility Phenotype in Transgenic Plants

None of the T1 plants of *Ugp1-OX* lines with a single T-DNA insertion showed any obvious phenotypic changes during the vegetative growth stage. However, during the reproductive growth stages, segregation was observed. All null segregants (PCR-negative) had a wild-type phenotype with normal fertility, whereas the PCR-positive transgenic T1 plants of the *Ugp1-OX* lines segregated into two subpopulations. The overexpressing subpopulation produced round, well-developed pollen grains and had a higher rate of seed-setting than the wild-type plants at maturity. In another cosuppressing subpopulation (Figure 3B), the panicle number was increased and the flowering time was delayed by several days compared with the wild-type Hejiang 19 plants (Table 1). They developed pale, shrunken anthers (Figures 3E and 3G), containing few collapsed and irregularly shaped pollen grains that adhered to each other and did not stain in the presence of KI-I_2 (Figure 3I). Consequently, these cosuppressing plants were completely male-sterile and bore no seeds on their panicles (Table 1).

Ugp1-RI plants showed pleiotropic developmental abnormalities (Figure 3C), including retarded growth, lower tiller numbers, reduced plant height, and delayed flowering (Table 1). When entering the reproductive stage, these plants also exhibited a male-sterile phenotype. Along with the male-sterility phenotype observed in cosuppressing plants, these results suggest that silencing of rice *Ugp1* led to male sterility in the transgenic rice.

Sterility was solely due to the defective male gametes; female fertility in the *Ugp1*-silenced plants (including *Ugp1-RI* and cosuppressing plants) was not affected. When the cosuppressing male-sterile plants were cross-pollinated with wild-type plants and other varieties, they produced normal seeds and the F1 plants exhibited normal fertility. When the male-sterile *Ugp1-RI* T0 plants carrying single T-DNA insertions were crossed with wild-type plants, the F1 plants segregated in a 1:1 fertile:male-sterile ratio, indicating that the male-sterility phenotype in the *Ugp1-RI* lines can be inherited and is only present in F1 individuals that carry the transgene.

Cosuppression and Male Sterility in *Ugp1-OX* Plants Occur Only When the Transgene Locus Is Homozygous

As shown in Table 2, T1 individuals from each *Ugp1-OX* T0 line with a single insertion segregated in a Mendelian fertile:sterile fashion, with a ratio of 3:1, suggesting that cosuppression of *Ugp1* and male sterility may be triggered in plants with a homozygous transgene locus. The 3:1 segregation ratio (Table 2) of fertile-to-sterile plants in the T2 progenies derived from T1 fertile transgenic plants indicates that these fertile T1 plants were heterozygous for the transgene locus. By contrast, all T2 progenies of null T1 segregants were fertile (Table 2). These fertility segregation analyses of T2 progenies further support the notion that cosuppression and its resulting male sterility are induced only in homozygotes, a previously documented phenomenon (de Carvalho et al., 1992). In addition, these results demonstrate that the male-sterility phenotype observed in the *Ugp1-OX* lines is attributable to the presence of the *Ugp1* transgene rather than to any pleiotropic effect of rice transformation and tissue culture.

Characterization of Male Gametogenesis in *Ugp1*-Silenced Plants

To clarify the nature of the male sterility in the *Ugp1*-silenced plants (including *Ugp1-RI* plants and cosuppressing plants),

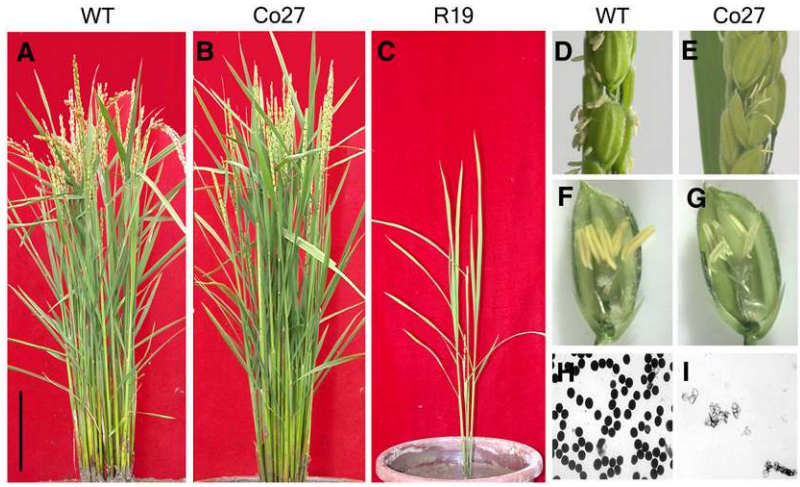

Figure 3. Phenotypes of *Ugp1*-Silenced Plants.

(A) Wild-type plant at maturity stage.
(B) Cosuppressing plant at maturity stage showing no seed set on the panicles.
(C) RNAi plant at maturity stage.
(D) Wild-type spikelets at the heading stage.
(E) Cosuppressing plant spikelets at the heading stage.
(F) Flower and anther morphology of a wild-type plant.
(G) Flower and anther morphology of a cosuppressing plant.
(H) Wild-type pollen grains stained with KI-I_2 solution.
(I) Cosuppressing plant pollen grains stained with KI-I_2 solution.
Co27, cosuppressing plant of line 27; R19, RNAi plant of line 19. Bar = 10 cm.

anther transverse sections were further examined. Based on the cellular events visible under the light microscope and the previous classification of anther development (Feng et al., 2001; Itoh et al., 2005), we delineated rice anther development into seven stages. Light microscopy observations indicated that the anther development was normal prior to meiosis of PMCs in *Ugp1*-silenced plants (exemplified by cosuppressing plants). Compared with wild-type anthers (Figure 4A), no differences were observed in the four outer layers (the epidermis, endothecium, middle layer, and tapetum) of the anther or PMCs of the cosuppressing plants before meiosis (Figure 4H). During the process of meiosis, the four outer layers of the anther remained normal (Figures 4I and 4J), but the PMCs of the cosuppressing plants began to degenerate in the locules of the anthers at an early stage of meiosis (Figure 4I). The degeneration continued into the later meiosis stage (Figure 4J). At the end of meiotic cell division, free microspores were released into the anther locules and the middle layers narrowed in the wild-type anthers (Figure 4D). By contrast, in the anthers of cosuppressing plants, the microspores were irregularly shaped and adhered to each other, and the middle layers retained their initial shape (Figure 4K).

Subsequently, in the later microspore stage, the microspores developed and the tapetum layers became very dense and thick in the wild-type anthers (Figure 4E). By contrast, in the cosuppressing plants, the microspores were shrunken and collapsed, and the tapetum layers began to manifest premature degeneration as the vacuoles enlarged (Figure 4L). At the pollen mitosis stage, the uninucleate pollen developed into trinucleate pollen through two mitotic divisions. In the wild-type plants, the tapetum layers were completely degenerated and the endothecial cell layers eventually ruptured, releasing the mature pollen grains (Figures 4F and 4G). At the same stage in anthers of cosuppressing plants, the pollen had completely degenerated, leaving only remnants in the anther locules, while the tapetum had become abnormally large and extremely vacuolated. The anthers also retained all four outer layers and did not dehisce (Figures 4M and 4N). These findings suggest that rice *Ugp1* is essential for PMCs meiosis and microspore development as early as the early meiosis stage. Moreover, this gene is needed for the degeneration of the tapetum and middle layer.

Callose Deposition Is Disrupted in Pollen of *Ugp1*-Silenced Plants

Pollen development involves dynamic turnover of cell wall layers and changes in their composition (Polowick and Sawhney, 1992; Owen and Makaroff, 1995). Previous studies have shown that callose, one of the cell wall components, appears to play a vital role in the process of pollen development, since the lack of callose affects proper pollen wall formation (Waterkeyn and Beinfait, 1970; Worrall et al., 1992; Dong, 2004; Dong et al., 2005). We reasoned that the degeneration and irregular shape of the pollen in *Ugp1*-silenced plants may be due to the loss of the *Ugp1* function in cell wall biosynthesis, which is required to maintain the integrity of the cell wall structure (Figures 4I to 4M). To test this possibility, we examined callose contents of the

Table 1. Morphological Characteristics of *Ugp1*-Silenced Plants

Line	Plant Height (cm)	Panicle Number	Flowering Time (Day)	Panicle Length (cm)	Grain Number (per Panicle)	Seed-Setting Rate (%)
Wild type	56.8 ± 2.01	24.0 ± 2.66	61.0 ± 0	13.4 ± 0.54	47.5 ± 2.23	75.9 ± 3.73
Co27[a]	54.8 ± 2.31	31.0 ± 4.02	65.7 ± 0.48	12.7 ± 1.53	48.3 ± 7.07	0
R19[b]	34.0 ± 6.34	6.0 ± 0.70	75.6 ± 2.07	11.5 ± 0.84	35.1 ± 4.17	0

Data represent means ± SE ($n = 10$).
[a] Co27, cosuppressing plant of line 27.
[b] R19, RNAi plant of line 19.

anthers at various developmental stages by aniline blue staining. Before the initiation of meiosis, callose was not detectable in PMCs of either wild-type or *Ugp1*-silenced plants (exemplified by cosuppressing plants; Figures 5A and 5E). At this stage, PMCs in cosuppressing plants appeared normal with no signs of degeneration (Figure 5E). During the process of meiosis, callose was deposited around the PMCs (seen as bright-yellow fluorescence in Figures 5B, 5C, 5F, and 5G) and the tetrads (Figures 5D and 5H). However, the PMCs and the tetrads of cosuppressing plants produced much less callose than those of wild-type plants and gradually degenerated (Figures 5F, 5G, and 5H). When microspores were released into the anther locule, both the normal microspores of the wild type and the degenerated microspores of cosuppressing plants exhibited weak callose fluorescence (Figures 5I and 5M). Subsequently, no callose signal was detected in the later microspores, binucleated pollens, or mature pollen of the wild-type plants (Figures 5J to 5L). However, strong callose fluorescence appeared in the abnormally large and extremely vacuolated tapetum of cosuppressing plants (Figures 5O and 5P). These results indicate that callose deposition was greatly reduced in the pollen (PMCs and tetrads) of cosuppressing plants during meiosis, and the lack of callose deposition due to cosuppression of *Ugp1* affected the pollen wall structure and viability of these plants.

UGPase Protein Accumulates in Pollen Cells throughout Pollen Development in Wild-Type Plants but Not in *Ugp1*-Silenced Plants

To gain further insight into the action of the UGPase protein, we analyzed its expression pattern in anthers at different stages using immunolocalization techniques. In the wild-type plants, the UGPase protein was located predominately in PMCs at the premeiosis stage (Figure 6A), the early meiosis stage (Figure 6B), and the subsequent meiosis stage (Figure 6C) but was not present in other anther tissues, such as the epidermis, endothecium, middle layer, and tapetum. UGPase protein signals were still detectable in microspores, but they gradually declined in strength (Figure 6D). In control sections treated with preimmune serum, only weak background signals were observed (Figure 6E). By contrast, when anthers at the premeiosis stage of *Ugp1*-silenced plants (exemplified by cosuppressing plants) were analyzed, only background signal levels were detected (Figure 6F). Therefore, these results strongly confirm that the expression of UGPase is associated with PMC meiosis and microspore development.

Male Sterility of Cosuppressing Plants Is a New Type of Thermosensitive Genic Male Sterility

While the male sterility of *Ugp1-RI* lines was stable under various environmental conditions, the cosuppressing plants that were completely sterile under natural summer conditions could revert to fertility in the autumn. When the cosuppressing plants headed in September, they showed normal fertility levels with seed setting 75.3% ± 1.47% ($n = 10$), equivalent to 75.9% of wild-type levels (Table 1). To determine if the male-sterility phenotype in T1 homozygous cosuppressing plants could be inherited by the seeds harvested in autumn, fertility parameters were also investigated in T2 progenies of these plants. As shown in Table 2, under natural summer conditions, the male sterility could be maintained through successive generations. Plants that were completely male-sterile in summer also reverted to fertility in autumn.

Table 2. Fertility of Transgenic Plants with a Single Insertion of *Ugp1-OX* and Their Progenies

Line	Fertile	Sterile	χ^2 (3:1)[a]
Segregation of fertility in *Ugp1-OX* T1 plants[b]			
10	9	4	0.2308
14	22	6	0.1905
27	20	3	1.7536
Segregation of fertility in T2 lines derived from heterozygous T1 plants[c]			
10-11	29	11	0.1333
14-8	96	30	0.0952
27-9	48	13	0.4426
Fertility in T2 lines derived from null segregant T1 plants[c]			
10-10	70	0	
14-1	90	0	
27-4	37	0	
Fertility in T2 lines derived from homozygous T1 plants[c]			
27-10	0	98	
27-12	0	38	
27-19	0	25	

[a] χ^2 values test the fit of counts of fertile/sterile progeny of T0 or T1 plants to a 3:1 ratio.
[b] The seeds from *Ugp1-OX* T0 plants of lines 10, 14, and 27 were soaked, sown, and transplanted on April 28, May 5, and May 27, 2004, respectively.
[c] These plants were soaked, sown, and transplanted on April 22, April 28, and May 14, 2005, respectively.

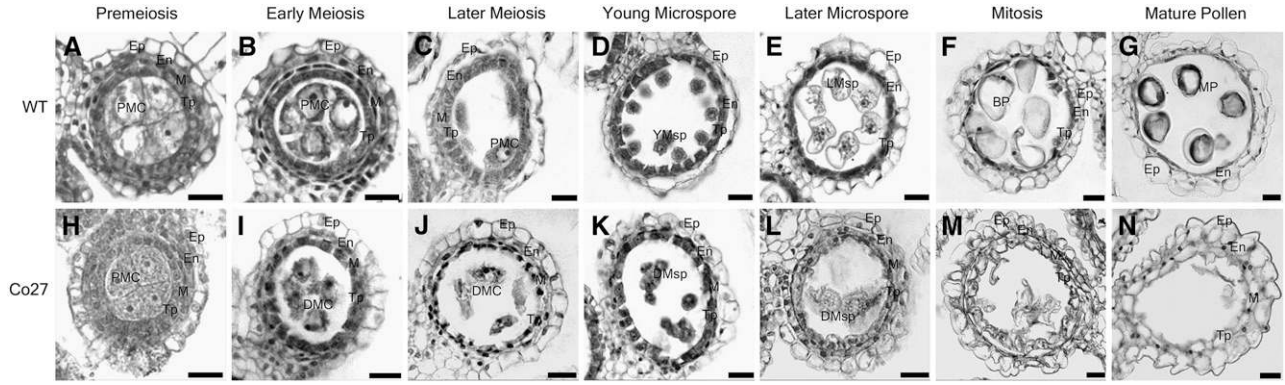

Figure 4. Anther Development in Wild-Type Plants and Cosuppressing Plants.

The micrographs show one of the four lobes in cross sections of wild-type anthers (**[A]** to **[G]**) and anthers from cosuppressing plants (**[H]** to **[N]**) at the premeiosis stage (**[A]** and **[H]**), early meiosis stage (**[B]** and **[I]**), meiosis stage (**[C]** and **[J]**), young microspore stage (**[D]** and **[K]**), later microspore stage (**[E]** and **[L]**), pollen mitosis stage (**[F]** and **[M]**), and mature pollen stage (**[G]** and **[N]**). DMC, degenerated meiocyte; Ep, epidermal cell layer; En, endothecial cell layer; M, middle layer; Tp, tapetum layer; YMsp, young microspore; DMsp, degenerated microspore; LMsp, later microspore; BP, binucleated pollen; MP, mature pollen. Bars = 10 μm.

The fertility reversion of cosuppressing plants followed a period of consistently low temperatures (≤21°C) and short daylength photoperiod (<12.5 h). These environmental parameters associated with the reversion to fertility in cosuppressing plants resemble those that trigger reversion in photoperiod-sensitive genic male-sterility and thermosensitive genic male-sterility (TGMS) lines, which have been widely used in hybrid rice seed production (Virmani et al., 2003). The photoperiod-sensitive genic male-sterility lines are stably sterile under long-day conditions (>13.75 h) but fertile under short-day conditions (<13 h), regardless of the temperature. By contrast, the TGMS lines are sensitive to temperature, since they retain male sterility at high temperatures (>27°C) but revert to fertility at low temperatures (<24°C) (Virmani et al., 2003). To determine whether the fertility reversion in cosuppressing plants is determined by the photoperiod, T2 progeny of cosuppressing plants were subjected to a short-day treatment (9-h-light/15-h-dark cycles) under natural summer conditions. The results showed that cosuppressing plants remained completely male-sterile under the short-day conditions, suggesting that the fertility transformation in the cosuppressing plants is controlled by temperature, not by the photoperiod. Thus, the male-sterility phenotype in cosuppressing plants is a new type of TGMS.

Temperature-Sensitive Splicing in Florets Is the Basis for Fertility Reversion of TGMS in Cosuppressing Plants

The fertility reversion of *Ugp1* cosuppressing plants at low temperature led us to hypothesize that the cosuppression of *Ugp1* in these plants might reset. In other words, the silenced gene may be reactivated, a well-documented characteristic of cosuppression (de Carvalho et al., 1992; Hart et al., 1992; Dorlhac de Borne et al., 1994). To test this possibility, we first investigated the expression of *Ugp1* in leaves of the fertility-reverted cosuppressing plants grown at low temperature (21°C). All fertility-reverted cosuppressing plants contained RNA degradation intermediates and the aberrant *Ubi1* intron-containing longer-than-full-length RNAs, and no signal was detected in the regions corresponding to endogenous *Ugp1* mRNA (Figure 7A). The expression of *Ugp1* was further analyzed in florets of the fertility-reversed cosuppressing plants at low temperature (21°C). The RNA samples were prepared from florets at different anther developmental stages, according to the previous classification of anther development (Feng et al., 2001; Itoh et al., 2005). The aberrant *Ubi1* intron-containing longer-than-full-length RNAs and RNA degradation intermediates were still present in florets of fertility-reversed cosuppressing plants, and endogenous *Ugp1* mRNAs were still completely suppressed (Figure 7B). These results indicate that cosuppression of *Ugp1* was still maintained in the fertility-reverted cosuppressing plants at low temperature (21°C).

The formation of organs and tissues usually requires the coordinated expression of a complex network of genes, and the function of the *Ugp1* gene in anther development may be replaced by other genes in cosuppressing plants at low temperature. This possibility is based on the hypothesis that the expression of UGPase protein in florets is also suppressed. Thus, to test this possibility, we analyzed the expression of UGPase protein in florets at various anther developmental stages by protein gel blot analysis. When cosuppressing plants were in the male-sterile stage under natural summer conditions (high temperature), they did not show any UGPase expression in florets of any of the developmental stages. Significantly, however, when they reverted to fertility in the autumn at low temperature (21°C), they accumulated UGPase protein in their florets at close to wild-type levels (Figure 7C). These findings indicate that fertility reversion in cosuppressing plants is due to the accumulation of UGPase protein in florets at low temperature (21°C). In contrast with the florets, UGPase protein expression remains unchanged in leaves of cosuppressing plants regardless of the temperature (Figure 7C).

In attempts to trace the source of the UGPase proteins that accumulated in florets of fertility-reverted cosuppressing plants

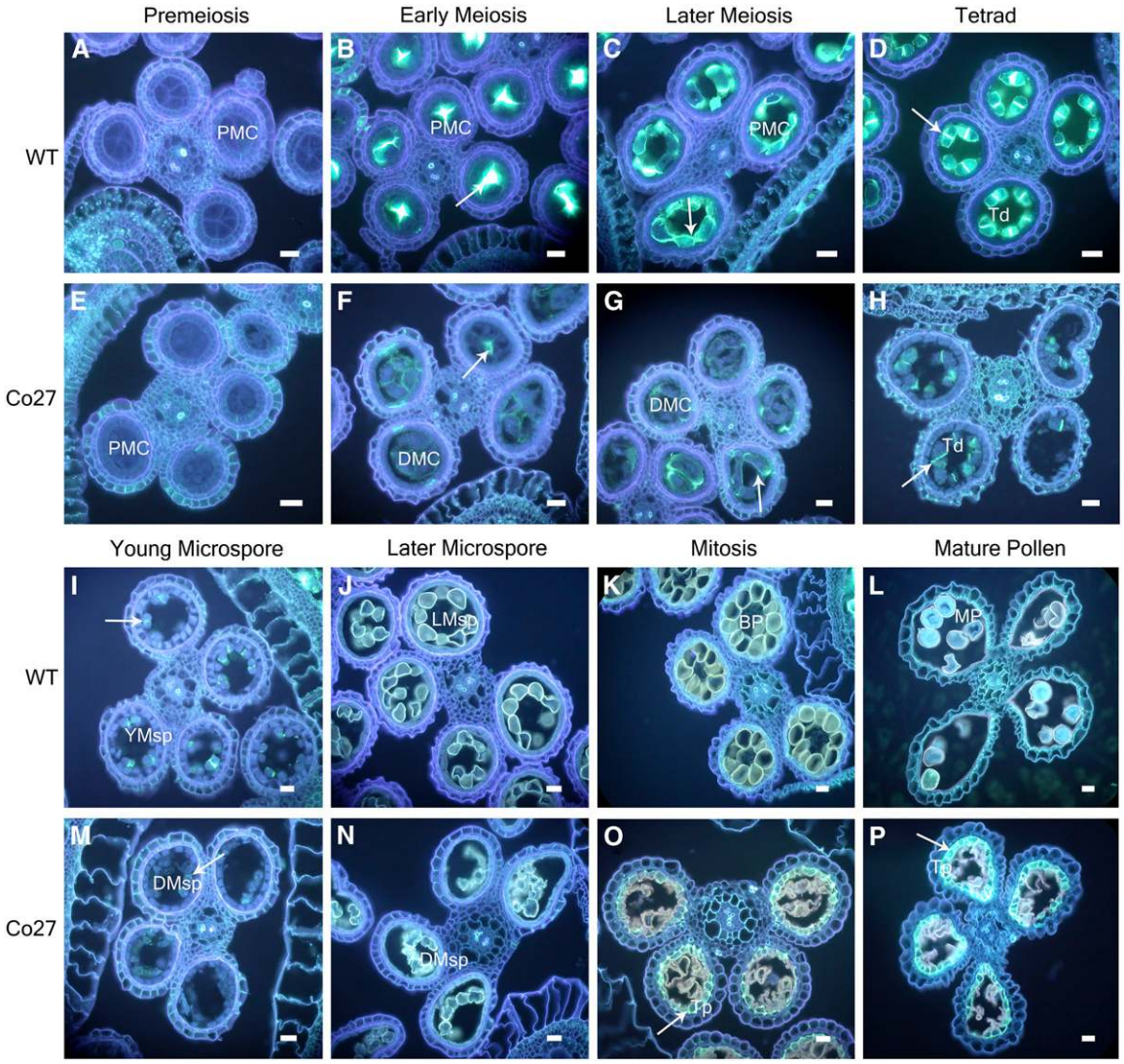

Figure 5. Callose Deposition in Anthers during Microsporogenesis.

Cross sections of wild-type anthers and anthers from cosuppressing plants were stained with aniline blue to detect callose. Wild-type sections are shown in **(A)** to **(D)** and **(I)** to **(L)**, and other panels show cosuppressing plant sections. Callose deposition is shown as bright-yellow fluorescence (indicated by arrows). Note that callose deposition was greatly reduced in PMCs and tetrads of cosuppressing plants. DMC, degenerated meiocyte; Td, tetrad; YMsp, young microspore; DMsp, degenerated microspore; LMsp, later microspore; BP, binucleated pollen; Tp, tapetum layer; MP, mature pollen. Bars = 10 μm.

(A) and **(E)** The premeiosis stage.
(B) and **(F)** The early meiosis stage.
(C) and **(G)** The later meiosis stage.
(D) and **(H)** The tetrad stage.
(I) and **(M)** The young microspore stage.
(J) and **(N)** The later microspore stage.
(K) and **(O)** The pollen mitosis stage.
(L) and **(P)** The mature pollen stage.

at low temperature (21°C), the possible contribution of endogenous *Ugp1* mRNA could be excluded since it was completely suppressed (Figure 7B). However, as shown in Figure 1B, *Ugp2* is also expressed in pooled florets at various stages before flowering. To determine whether the expression of *Ugp2* contributes to the accumulation of UGPase proteins observed in florets of fertility-reverted cosuppressing plants at low temperature, we analyzed *Ugp2* expression by RT-PCR of total RNA extracted from florets at different anther developmental stages. PCR primers were designed based on the 5′- and 3′-untranslated

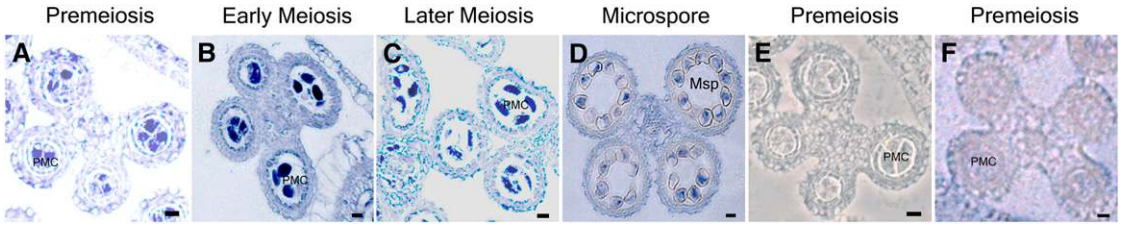

Figure 6. Expression of UGPase Protein in Wild-Type Anthers and Cosuppressing Anthers.

UGPase protein was immunolocalized in anthers of wild-type plants (**[A]** to **[E]**) and cosuppressing plants **(F)**. The blue staining in the anthers of the wild-type plants at the premeiosis stage **(A)**, early meiosis stage **(B)**, later meiosis stage **(C)**, and microspore stage **(D)** shows the localization of the UGPase protein in the PMCs and microspores. A consecutive section of **(A)** treated with preimmune serum as a negative control **(E)**. No UGPase protein was detected in the anthers of cosuppressing plants at the premeiosis stage **(F)**. Msp, microspore. Bars = 10 μm.

regions of *Ugp2* to amplify full-length fragments of *Ugp2* cDNA. As shown in Figure 7D, *Ugp2* was mainly expressed in florets in the pollen mitosis stage, and the expression of *Ugp2* was not affected in florets of cosuppressing plants, regardless of whether the temperature was high or low. Thus, the possible contribution of *Ugp2* to the accumulation of UGPase proteins in florets of fertility-reverted cosuppressing plants at low temperature could also be excluded.

The aberrant longer-than-full-length RNAs, which contained the unspliced intron in the 5′-untranslated region of the *Ubi1* promoter (Figures 7A and 7B), are unprocessed primary transcripts derived from the transcription of the *Ugp1-OX* construct (Figure 2A). These molecules in cosuppressing plants are destined to be processed for degradation or, alternatively, for processing into mature RNAs for translation, possibly contributing to the accumulation of UGPase proteins in florets of fertility-reverted cosuppressing plants at low temperature. To test the latter possibility, we performed RT-PCR to analyze the correctly spliced *Ugp1* mRNAs from longer-than-full-length RNAs in florets of cosuppressing plants. As shown in Figure 7D, RT-PCR amplification of the correctly spliced *Ugp1* mRNA sequence between the exon of the *Ubi1* promoter and the 3′-untranslated regions of the nopaline synthase (Nos) terminator revealed the predicted 1521-bp product in florets of cosuppressing plants, both at high temperature and low temperature. Florets of cosuppressing plants that developed at low temperature accumulated much more correctly spliced *Ugp1* mRNAs from longer-than-full-length RNAs than florets that developed at high temperature (Figure 7D). This finding shows that splicing of *Ugp1* mRNA is temperature sensitive. Taken together, the results described above demonstrate that temperature-sensitive splicing of *Ugp1* mRNAs from longer-than-full-length RNAs contributes to the accumulation of UGPase proteins in florets of cosuppressing plants, which is the molecular basis of the TGMS fertility reversion in cosuppressing plants.

DISCUSSION

UGPase Is Essential for Growth and Development in Rice

UGPase is a key enzyme in plant carbohydrate metabolism and cell wall biosynthesis that catalyzes the reversible production of glucose-1-phosphate and UTP to UDP-glucose and pyrophosphate. It has been well established that UGPase is essential for normal cell physiology and development in yeast and other fungi (Dimond et al., 1976; Daran et al., 1995; Bishop et al., 2002). However, reductions of UGPase activity in potato and *Arabidopsis* by antisense suppression have been shown to have no detectable effect on plant growth and development (Zrenner et al., 1993; Spychalla et al., 1994; Borovkov et al., 1996; Johansson, 2003). In this study, although silencing of *Ugp1* by cosuppression also had no visible phenotypic effects on rice during vegetative growth, when *Ugp1* was silenced by expressing a dsRNAi construct, pleiotropic developmental abnormalities (including retarded growth, lower tiller numbers, reduced plant height, and delayed flowering) occurred (Table 1, Figure 3C), providing direct evidence that UGPase plays critical roles in plant growth and development.

The failure to detect growth and developmental defects in previous antisense studies in potato and *Arabidopsis* was very likely due to low suppression efficacy and the presence of other *Ugp* genes. The phenotypic differences in vegetative growth between *Ugp1-RI* plants and cosuppressing plants may also result from the different silencing efficacy. Cosuppression of *Ugp1* has no effect on the expression of *Ugp2*; however, both *Ugp1* and *Ugp2* are completely suppressed in *Ugp1-RI* plants (Figure 7D). Generally, the genetic requirements for S-PTGS (cosuppression) and IR-PTGS (dsRNAi) are different, and dsRNA is the branch point between the S-PTGS and IR-PTGS pathways. AGO1, SGS2/SDE1, SGS3, and SDE3 proteins, which are required for the formation and/or replication of dsRNA in S-PTGS, are dispensable for IR-PTGS (Beclin et al., 2002). The high efficiency of IR-PTGS is due to the folding of transgene-derived RNAs into long, stable dsRNA structures (Wesley et al., 2001). Thus, dsRNA is constitutively produced and the endogenous *Ugp* mRNAs, including *Ugp1* and *Ugp2*, are degraded globally in *Ugp1-RI* plants (Wesley et al., 2001; Baulcombe, 2004), resulting in severe vegetative growth defects that are absent in cosuppressing plants.

Rice *Ugp1* Is Required for Callose Deposition during Pollen Development

Ugp1-silenced plants (including *Ugp1-RI* plants and cosuppressing plants) are male-sterile but female-fertile. During meiosis,

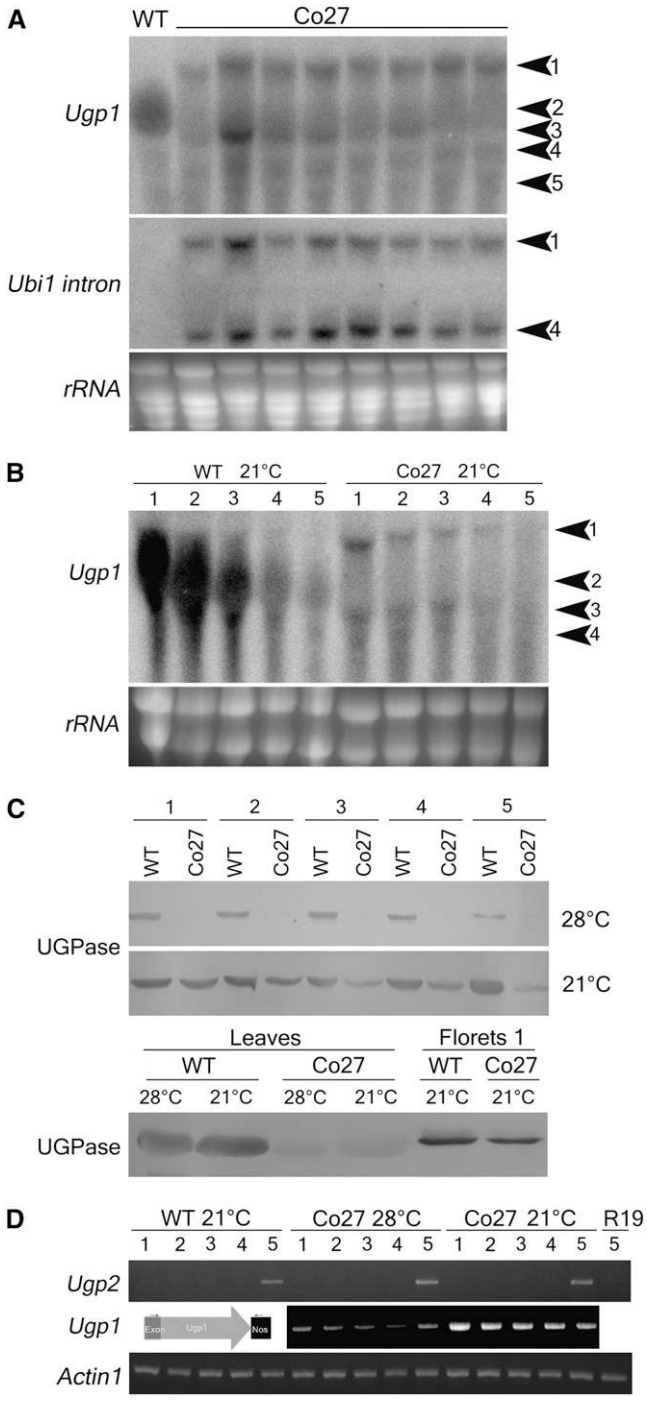

Figure 7. Effects of Temperature on Expression of *Ugp1* and *Ugp2* in Cosuppressing Plants.

The numbers above the lanes indicate the following anther developmental stages: 1, premeiosis; 2, meiosis; 3, young microspore; 4, later microspore; and 5, pollen mitosis. Co27, cosuppressing plant of line 27; R19, RNAi plant of line 19.

(A) RNA gel blot analysis of *Ugp1* transcript levels in leaves of fertility-reverted cosuppressing plants at low temperature. The RNA gel blot was hybridized with the corresponding *Ugp1* and subsequently with the *Ubi1* intron probes. Arrowheads indicate (1) the unprocessed longer-than-full-length transcript and (2) endogenous *Ugp1* mRNA; (3) to (5) indicate the silencing-related RNA degradation intermediates. Loading of equal amounts of RNA was confirmed by ethidium bromide staining.

(B) RNA gel blot analysis of *Ugp1* transcript levels in florets of fertility-reverted cosuppressing plants grown at low temperature. The RNA gel blot was hybridized with corresponding *Ugp1* probes. Loading of equal amounts of RNA was confirmed by ethidium bromide staining.

(C) Protein gel blot analysis of UGPase protein in cosuppressing plants. Protein samples were extracted from florets and leaves of cosuppressing plants grown at high temperature (male sterile stage) and low temperature (male fertile stage).

(D) RT-PCR analysis of the expression of *Ugp2* and correctly spliced *Ugp1* from unprocessed primary transcripts derived from transcription of the *Ugp1-OX* construct (Figure 2A) in florets of cosuppressing plants. Amplification of the rice *Actin1* gene was used as a control to show that approximately equal amounts of total RNA had been used in the RT-PCR analysis.

normal callose deposition was disrupted in the PMCs of *Ugp1*-silenced plants (Figures 5F to 5H), resulting in their degeneration at the early stage of meiosis. The results demonstrated here provide direct evidence that rice *Ugp1* is essential for callose deposition during pollen development. Consequently, only the remnants of pollen remain in the locules of *Ugp1*-silenced plants' anthers. The anthers of *Ugp1*-silenced plants also show other developmental defects. While the middle layer and the tapetum degenerate in the wild-type anthers, this process does not occur in *Ugp1*-silenced plants' anthers.

Multiple roles for the callose wall have been proposed over the last 40 years. Prior to meiosis, the sporogenous initials divide to form PMCs surrounded by a simple primary wall with a distinct middle lamella. The wall doubles in width, and newly formed fibrillar wall materials are deposited in it. At the onset of meiosis, the wall microfibrils disappear and a secondary callose wall is deposited between the primary wall and plasma membrane of the PMCs (Polowick and Sawhney, 1992; Owen and Makaroff, 1995). The callose layer is believed to prevent the cohesion and fusion of the PMCs (Waterkeyn, 1962), and it may function as a molecular filter that protects the developing pollen cells from premature swelling and bursting under the influence of the surrounding diploid tissues (Heslop-Harrison and Mackenzie, 1967). In addition, the callose wall can provide a template or mold for formation of the exine wall of pollen grains (Waterkeyn and Beinfait, 1970; Worrall et al., 1992; Dong, 2004; Dong et al., 2005). The *Arabidopsis* callose synthase mutant *cals5* lacks normal callose deposition in meiocytes, tetrads, microspores, and mature pollen. Consequently, the pollen exine wall is not formed properly and the mutant exhibits male sterility (Dong et al., 2005). However, *cals5* mutants undergo apparently normal meiosis. Similarly, normal callose deposition was disrupted in PMCs of *Ugp1*-silenced plants in our study, but this led to degeneration of the PMCs at the early stage of meiosis. Our results demonstrate that callose deposition is also essential for both the integrity of PMC cell walls and male meiosis, in addition to the other important roles of callose deposition in the process of microsporogenesis (Tucker et al., 2001; Dong et al., 2005).

In plants, UDP-glucose can potentially be synthesized by two different pathways. One pathway involves UGPase, while the second involves SuSy, which catalyzes the reversible hydrolysis of sucrose to fructose and UDP-glucose. A membrane-associated form of SuSy has been suggested to channel carbon directly from sucrose to cellulose and/or callose in developing cotton fibers (Amor et al., 1995). However, the developing pollen represents a symplastically isolated sink with no plasmodesmatal connections to the surrounding sporophytic tissue (Clément and Audran, 1995). Thus, an unloading pathway via apoplastic cleavage of sucrose by extracellular invertase and uptake of the resulting hexose monomers by monosaccharide transporter is mandatory (Eschrich, 1980). It has been reported that invertase is the dominant sucrose-cleaving enzyme in anthers (Dorion et al., 1996; Sheoran and Saini, 1996; Ranwala and Miller, 1998; Koonjul et al., 2005). In wheat (*Triticum aestivum*) and rice, the arrest of pollen development and consequent male sterility by meiotic-stage water stress is preceded by a specific decline in anther invertase activity, resulting from selective transcriptional downregulation of anther invertase genes (Dorion et al., 1996; Sheoran and Saini, 1996; Koonjul et al., 2005). Tissue-specific antisense inhibition of the extracellular invertase gene *Nin88* under the control of its own promoter in tobacco (*Nicotiana tabacum*) reduces apoplastic invertase activity, leading to the developmental arrest of pollen at the unicellular microspore stage, thus causing male sterility (Goetz et al., 2001). Furthermore, cold-induced repression of the rice anther-specific cell wall invertase gene Os *INV4* is correlated with the significant reduction in anther cell wall–bound invertase activity, premature callose degradation, and eventual pollen sterility (Oliver et al., 2005; Mamun et al., 2006). Taken together, these results (and the identification of the pollen-specific monosaccharide transporter; Ylstra et al., 1998; Truernit et al., 1999) prove that the apoplastic unloading pathway plays a vital role in pollen development. In this context, rice *Ugp1* could bridge the apoplastic unloading pathway and pollen development because it is specifically expressed in pollen cells during anther and pollen development (Figure 6). Briefly, in the anther apoplastic unloading pathways, sucrose is irreversibly hydrolyzed by extracellular invertase. The resulting hexose monomers are taken up by pollen cells through pollen-specific monosaccharide transporters (Ylstra et al., 1998; Truernit et al., 1999) and then metabolized to glucose-1-phosphate, which is converted to UDP-glucose by UGPase for pollen cell wall biosynthesis.

Temperature-Sensitive Splicing in Florets Is the Basis for Fertility Reversion of TGMS in Cosuppressing Plants

Cosuppression was originally discovered as the reciprocal and coordinated silencing of transgenes and homologous host genes (Napoli et al., 1990; van der Krol et al., 1990). It is more pronounced in homozygous than in corresponding hemizygous plants (de Carvalho et al., 1992; Hart et al., 1992; Dorlhac de Borne et al., 1994). The frequency of cosuppression positively correlates with the promoter strength of the transgene (Que et al., 1997). In addition, transgene transcription is required for cosuppression (Dorlhac de Borne et al., 1994; Vaucheret et al., 1997). In this study, the *Ugp1* transgene was under the control of the strong, constitutive maize *Ubi1* promoter, and cosuppression was triggered exclusively when plants were homozygous for the transgene locus. Both of these findings support the cosuppression threshold hypothesis (Lindbo et al., 1993). Significantly, in addition to low molecular weight and silencing-related RNA degradation intermediates, aberrant *Ubi1* intron-containing longer-than-full-length *Ugp1* mRNAs, which are unprocessed primary transcripts derived from transcription of the *Ugp1-OX* construct (Figure 2A), were present in the cosuppressing plants (Figure 7A). This can be attributed to the characteristics of the *Ubi1* promoter that drives the *Ugp1* expression. The *Ubi1* promoter of maize contains two overlapping sequences similar to the consensus heat shock element found in heat-inducible genes and an intron (Figure 2A). The heat shock elements of the promoter region enhance the expression of the downstream gene in response to elevated temperatures, and the intron is inefficiently processed following a brief, severe heat shock (Christensen et al., 1992).

Recently, it has been shown that low temperature inhibits virus- and transgene-induced RNA silencing by controlling siRNA generation, leading to enhanced virus susceptibility and loss of silencing-mediated transgenic phenotypes. By contrast, RNA silencing is activated and the amount of siRNAs gradually increases with rising temperature (Szittya et al., 2003). However, our results indicate that cosuppression of *Ugp1* was not affected in fertility-reverted cosuppressing plants at low temperature (Figures 7A and 7B). Significantly, temperature strongly affected the splicing of *Ugp1* mRNAs from longer-than-full-length RNAs. Florets of cosuppressing plants grown at low temperature accumulated much more correctly spliced *Ugp1* mRNAs from longer-than-full-length RNAs than those grown at high temperature (Figure 7D), which contributed to the accumulation of sufficient levels of UGPase protein in their florets and, thus, their reversion to fertility. Our results demonstrate that the TGMS phenotype of the cosuppressing plants is attributable to temperature-sensitive splicing, which may provide clues regarding other unknown, molecular TGMS mechanisms (Kurata et al., 2005).

Several types of temperature-sensitive mutations affecting splicing have been characterized. These mutations affect *trans*-acting proteins required for pre-mRNA splicing due to the production of a defective protein product (Weidenhammer et al., 1996; Arenas and Abelson, 1997). There are few reported cases of temperature-sensitive mutations that have a *cis* effect on the splicing of a specific transcript (Hughes et al., 1996; Sablowski and Meyerowitz, 1998; Gemignani et al., 2002). The temperature-sensitive mutant *ap3-1* carries a missense mutation near a 5′-splice site in exon 5. At the nonpermissive temperature, exon 5 is frequently skipped by the splicing machinery. The resulting inactive AP3De5 causes *ap3-1* to develop sepaloid organs and carpelloid organs instead of stamens. At the permissive temperature, the correctly spliced *ap3-1* mRNA (exon 5–containing mRNA) accumulates, and the presence of sufficient levels of the active missense mutation protein AP3–Met-153 allows *ap3-1* to produce nearly wild-type flowers (Sablowski and Meyerowitz, 1998). Similarly to *ap3-1* mutant, the temperature-sensitive splicing of *Ugp1* from transgene transcripts in cosuppressing plants could also be attributable to the temperature sensitivity of

a component of the splicing machinery. More interestingly, the temperature-sensitive splicing of *Ugp1* in cosuppressing plants provides a novel example of *cis* element (heat shock element) based temperature-sensitive splicing, which may involve the interactions of heat shock elements, heat shock transcription factors, and heat shock proteins (Yost and Lindquist, 1986, 1991).

METHODS

Plant Materials

The wild-type rice (*Oryza sativa*) strain used in this study was a japonica variety, Hejiang 19. The transgenic plants and wild-type plants were grown in an experimental field at Wuhan University Institute of Genetics (Wuhan, China) (latitude 30°34' North; longitude 114°17' East). All experimental materials were transplanted in the field at a spacing of 16.7 cm between plants within each row and 26.7 cm between rows. The plants were tended under the routine management regime.

Plasmid Constructs and Plant Transformation

All constructs were made using standard procedures (Sambrook et al., 1989). Enzymatic reactions were performed using the conditions and buffers recommended by the suppliers. Plasmid pAHC17 (Christensen and Quail, 1996) was partially digested with *Hin*dIII and *Eco*RI. The maize (*Zea mays*) ubiquitin 1 (*Ubi1*) promoter and Nos terminator cassette were inserted into the *Hin*dIII and *Eco*RI sites of pCAMBIA 1301, resulting in plasmid pCU. The coding region of rice *Ugp1* was amplified using primers 5′-ATTGGATCC*ATG*GCGGTCGCCGCCGACGTG-3′ and 5′-CCGGGATCC*TCA*AAGATCCTCCGGACCGTTG-3′ and ligated to the *Bam*HI site of pCU to make the overexpression construct (*Ugp1-OX*) and antisense construct (*Ugp1-AS*), respectively (Figure 2A). The *Ugp1-OX* and *Ugp1-AS* constructs were confirmed by sequencing.

To make a dsRNAi construct, a 520-bp fragment between +333 and +852 (related to the ATG at +1 bp) was amplified from the *Ugp1* coding sequence using the following primers: 5′-CCTCTCGAGCCTTATTGTGATTCAAATTGAG -3′ (*Xho*I), 5′-CTTGAATTCATTCACATGCTCATC-3′ (*Eco*RI), 5′-GTTTCTAGACCTTATTGTGATTC-3′ (*Xba*I), and 5′-CTTAAGCTTATTCACATGCTCATCAGGGAC-3′ (*Hin*dIII). The PCR fragment generated using the *Xho*I-*Eco*RI pair of primers (to form the sense fragment) was cloned first into pGEM-T (Promega), and then the *Xho*I-*Eco*RI–digested *Ugp1* fragment was cloned into the same restriction enzyme sites present in the pKANNIBAL vector (Wesley et al., 2001), thus creating pKAN-*Ugp1*XE. The PCR fragment generated using the *Xba*I-*Hin*dIII pair of primers (to form the antisense fragment) was also cloned first into pGEM-T vector, and then the *Xba*I-*Hin*dIII–digested *Ugp1* fragment was cloned into the same sites in pKAN-*Ugp1*XE to create pKAN-$(Ugp1)_2$. The *Xba*I-*Xho*I dsRNAi fragment contained the two *Ugp1* sequences in opposing orientations separated by an 800-bp *Pdk* intron sequence. This dsRNAi fragment was amplified using the following primers, with the added *Bam*HI site underlined, 5′-ATTGGATCCATTTGGAGAGGACACGCTCGAG-3′ and 5′-CTCGGATCCCTCATTAAAGCAGGACTCTAG-3′. It was then ligated to the *Bam*HI site of pCU to form the dsRNAi construct (*Ugp1-RI*, Figure 2A). Overexpression, antisense, and dsRNAi constructs were introduced into *Agrobacterium tumefaciens* (strain EHA105) by electroporation. The *Agrobacterium*-mediated transformation was performed using vigorously growing calli derived from mature embryos of Hejiang 19 following a standard procedure (Hiei et al., 1994). T0 transgenic plants were grown in a greenhouse under 14-h-light/10-h-dark cycles at 28°C.

Molecular Analyses

Total RNA was isolated using TRIzol reagent (Gibco BRL) according to the manufacturer's protocol from various rice tissues: roots, seedling stems, mature stems, seedling leaves, mature leaves, and florets. The florets at different anther developmental stages were classified in the following categories according to floret length (Feng et al., 2001; Itoh et al., 2005): premeiosis, meiosis, young microspore, later microspore, and pollen mitosis stages when the floret length was 1 to 2, 2 to 3, 3 to 4, 4 to 5, and 5 to 7 mm, respectively. RNA concentrations were estimated based on absorbance at 260 and 280 nm. For RNA gel blot analysis, total RNA was separated on a denaturing 1.5% formaldehyde agarose gel (Sambrook et al., 1989). Loading of equal amounts of RNA was confirmed by ethidium bromide staining. The RNA was transferred to Hybond N^+ membrane (Amersham Pharmacia Biotech). The probe was labeled with [α-^{32}P]dCTP using the Prime-a-Gene labeling system (Promega), and the membranes were hybridized for at least 10 h at 65°C with the labeled probe. Blots were washed for 15 min at 65°C in 1× SSC and 0.2% SDS and subsequently for 15 min at 65°C in 0.5× SSC and 0.1% SDS. The membranes were then exposed to x-ray film for autoradiography.

siRNA detection was performed as previously described (Lechtenberg et al., 2003). Electrophoresis was performed in 3% agarose gels in the presence of formaldehyde. Blots of siRNAs were prehybridized at 58°C for 2 h, and hybridizations were performed at 42°C for 16 h. The blots were washed for 3× 10 min at 37°C in 2× SSC/0.5% SDS and then in 2× SSC/0.2% SDS at 42°C for 10 min. The *Ugp1* primers (18 and 21 nucleotides) were used as size standard and hybridization controls.

For RT-PCR analysis, 2 μg of total RNA, extracted as described above, was treated with RQI RNase-Free DNase I (Promega) and then reverse-transcribed in a total volume of 20 μL using the Superscript III first-strand cDNA synthesis system for RT-PCR and oligo$(dT)_{20}$ primer according to the manufacturer's instructions (Invitrogen). The 20-μL first-strand cDNA product was diluted to 100 μL final volume with TE buffer, and 1 μL of the resulting dilutions was used as template in a 25-μL reaction mixture with the KOD Plus DNA polymerase (TOYOBO) using gene-specific primers. Two primers, 5′-TCATCAGATCAGCGTGAAGC-3′ and 5′-GCCCACTCACAAGGAGAAAA-3′, based on the 5′- and 3′-untranslated regions of rice *Ugp2*, were used to amplify the full-length fragments of *Ugp2* cDNA. For the analysis of spliced *Ugp1* from unprocessed primary transcripts derived from the *Ubi1* promoter, primer pair *Ubi1* exon-F (5′-AACCAGATCTCCCCCAAATC-3′) and Nos-R (5′-AAGACCGGCAACAGGATTC-3′), based on the 83-bp leader sequence adjacent to the transcription start site (exon) of the *Ubi1* promoter and 3′-untranslated regions of Nos terminator (Figure 2A), were used. For amplification of the rice *Actin1* gene, primer pair Actin1-F (5′-GAACTGGTATGGTCAAGGCTG-3′) and Actin1-R (5′-TCCAACACAATACCTGTGGT-3′) were used. The number of cycles used for amplification with each primer pair was adjusted to ensure that the amplification was in the linear range. The PCR products were sequenced to ensure that they were derived from the targeted genes.

UGPase Enzyme Activity Assay

Protein extraction was performed as previously described (Ciereszko et al., 2001a). Rice leaves and florets at various developmental stages were ground to powder with liquid nitrogen and homogenized in extraction buffer with a sample-to-buffer ratio of 1:5 (w/v). The homogenate was centrifuged for 15 min at 20,000*g* at 4°C, and the resulting supernatant was used to assay UGPase activity (Sowokinos et al., 1993). Reaction mixtures (1 mL, pH 8.5) contained 80 pmol of glycylglycine, 1 pmol of UDP-Glc, 5 pmol of $MgC1_2$, 1 unit each of phosphoglucose mutase and Glc-6-P dehydrogenase, 20 pmol of Cys, 0.02 pmol of Glc-1,6-diP, 0.6 pmol of NADP, and 20 μL of protein extract. The reactions were initiated by the addition of 2.5 pmol of inorganic pyrophosphate. The formation of NADPH (340 nm) was recorded continuously at 30°C until the reaction rate was no longer linear. One unit of

activity in the pyrophosphorolysis direction was defined as the amount of enzyme that catalyzes the formation of 1 μmol of Glc-1-P/min.

Protein Gel Blot Analysis

Eight microliters of sample extract was mixed with 2 μL of 5× SDS-PAGE sample buffer (Sambrook et al., 1989). Samples were heated for 3 min at 95°C and loaded on 12% SDS-polyacrylamide gels. After electrophoresis, proteins were electroblotted to nitrocellulose membranes. Membranes were blocked in 5% nonfat dry milk in TBS-T (20 mM Tris-HCl, pH 7.6, 137 mM NaCl, and 0.1% Tween 20) overnight at 4°C and then washed three times in TBS-T for 8 min each. The membranes were incubated with the primary UGPase polyclonal antibody (1:2500) diluted with 1% BSA in TBS-T for 1 h at room temperature (Chen et al., 2007). Next, the membranes were washed in TBS-T three times for 8 min each. Membranes were then incubated for 1 h with goat anti-rabbit IgG (1:2500 dilution in TBS-T and 1% BSA) conjugated to alkaline phosphatase, followed by three washes for 8 min each in TBS-T, and detected using the 5-bromo-4-chloro-3-indolyl phosphate/nitroblue tetrazolium (BCIP/NBT) solution as the substrate.

Histological Analysis

Bright-field photographs of individual flowers were taken using an Olympus SZX12 dissecting microscope equipped with CCD. Rice anthers at various developmental stages were dissected and vacuum infiltrated with 4% paraformaldehyde in PBS, pH 7.0, for 30 min, and then the fixative was renewed with fresh paraformaldehyde solution and left to fix at 4°C overnight. The samples were washed in PBS, dehydrated in a graded ethanol series, and embedded in Paraplast Plus (Sigma-Aldrich). Microtome sections (10 μm thick) were stained with 0.2% hematoxylin to stain the cells and 0.1% aniline blue to stain the callose walls. The slides were inspected and photographed using an Olympus BX51 microscope.

For immunocytochemical analysis, the sections were washed six times, after dewaxing and rehydration, in PBST (PBS and 0.05% Tween 20). After blocking for 30 min in 0.5% BSA and 10% normal goat serum in PBST at room temperature, the slides were incubated overnight with a 1:1000 dilution of the primary UGPase polyclonal antibody in PBST and 0.5% BSA at 4°C. The slides were then washed six times in PBST and incubated for 30 min at 37°C with a 1:500 dilution of the secondary antibody (alkaline phosphatase–conjugated goat anti-rabbit antibody). Subsequently, the slides were washed six times in PBST and developed with BCIP/NBT in TNM (10 mM Tris-HCl, pH 9.5, 100 mM NaCl, and 5mM $MgCl_2$). Sections were examined and photographed using a cooled CCD on an Olympus BX51 microscope.

Fertility Investigation

The anthers of the wild-type and transgenic plants were collected from spikelets just before anthesis. Pollen grains from the broken anthers were suspended in a 1% iodine–potassium iodide solution (KI-I_2). The stained pollen was examined and photographed under a microscope (Olympus BX51). To investigate seed setting, panicles were bagged before heading to prevent cross-pollination. The spikelets and grains from each of the panicles were counted.

Accession Numbers

Sequence data from this article can be found in the GenBank/EMBL data libraries under accession numbers DQ395328 (*Ugp1*) and AF249880 (*Ugp2*).

Supplemental Data

The following material is available in the online version of this article.

Supplemental Figure 1. UGPase Activity Assay in *Ugp1-RI* T0 Plants.

ACKNOWLEDGMENTS

We thank Chonglie Ma (University of Arizona) for critical comments on the manuscript. We also thank Peter Quail (USDA–Agricultural Research Service, Albany, CA) for providing us with the pAHC17 plasmid, Peter M. Waterhouse (Commonwealth Scientific and Industrial Research Organization Plant Industry, Canberra, Australia) for the gift of the pKANNIBAL vector, and T. John Andrews (Australian National University) for providing the Rubisco antibody. We thank Kaihua Wei (National Center of Biomedical Analysis, China) for specialized Q-TOF MS/MS analysis and Heping Li (Huazhong Agricultural University, China) for discussions about the results of the cytological observations. This work was supported by grants from the National Special Key Project on Functional Genomics and Biochip of China (2005AA2Z1021 and 2006AA10A103) and by the Program for Changjiang Scholars and Innovative Research Team in the University of China from the National Natural Science Foundation of China (30521004).

Received June 7, 2006; revised March 1, 2007; accepted March 15, 2007; published March 30, 20007.

REFERENCES

Abe, T., Niiyama, H., and Sasahara, T. (2002). Cloning of cDNA for UDP-glucose pyrophosphorylase and the expression of mRNA in rice endosperm. Theor. Appl. Genet. **105:** 216–221.

Amor, Y., Haigler, C.H., Johnson, S., Wainscott, M., and Delmer, D.P. (1995). A membrane-associated form of sucrose synthase and its potential role in synthesis of cellulose and callose in plants. Proc. Natl. Acad. Sci. USA **92:** 9353–9357.

Arenas, J.E., and Abelson, J.N. (1997). Prp43: An RNA helicase-like factor involved in spliceosome disassembly. Proc. Natl. Acad. Sci. USA **94:** 11798–11802.

Baulcombe, D. (2004). RNA silencing in plants. Nature **431:** 356–363.

Beclin, C., Boutet, S., Waterhouse, P., and Vaucheret, H. (2002). A branched pathway for transgene-induced RNA silencing in plants. Curr. Biol. **12:** 684–688.

Bishop, J.D., Moon, B.C., Harrow, F., Ratner, D., Gomer, R.H., Dottin, R.P., and Brazill, D.T. (2002). A second UDP-glucose pyrophosphorylase is required for differentiation and development in *Dictyostelium discoideum*. J. Biol. Chem. **277:** 32430–32437.

Borovkov, A.Y., McClean, P.E., Sowokinos, J.R., Ruud, S.H., and Secor, G.A. (1996). Effect of expression of UDP-glucose pyrophosphorylase ribozyme and antisense RNAs on the enzyme activity and carbohydrate composition of field-grown transgenic potato plants. J. Plant Physiol. **147:** 644–652.

Chen, R., Zhao, X., Shao, Z., Zhu, L., and He, G. (2007). Multiple isoforms of UDP-glucose pyrophosphorylase in rice. Physiol. Plant. **129:** 725–736.

Christensen, A.H., and Quail, P.H. (1996). Ubiquitin promoter-based vectors for high-level expression of selectable and/or screenable marker genes in monocotyledonous plants. Transgenic Res. **5:** 213–218.

Christensen, A.H., Sharrock, R.A., and Quail, P.H. (1992). Maize polyubiquitin genes: Structure, thermal perturbation of expression and transcript splicing, and promoter activity following transfer to protoplasts by electroporation. Plant Mol. Biol. **18:** 675–689.

Ciereszko, I., Johansson, H., Hurry, V., and Kleczkowski, L.A. (2001a). Phosphate status affects the gene expression, protein content and enzymatic activity of UDP-glucose pyrophosphorylase in wild-type and pho mutants of *Arabidopsis*. Planta **212:** 598–605.

Ciereszko, I., Johansson, H., and Kleczkowski, L.A. (2001b). Sucrose and light regulation of a cold-inducible UDP-glucose pyrophosphorylase gene via a hexokinase-independent and abscisic acid-insensitive pathway in *Arabidopsis*. Biochem. J. **354:** 67–72.

Clément, C., and Audran, J.C. (1995). Anther wall layers control pollen sugar nutrition in *Lilium*. Protoplasma **187:** 172–181.

Daran, J.M., Dallies, N., Thines-Sempoux, D., Paquet, V., and Francois, J. (1995). Genetic and biochemical characterization of the UGP1 gene encoding the UDP-glucose pyrophosphorylase from *Saccharomyces cerevisiae*. Eur. J. Biochem. **233:** 520–530.

de Carvalho, F., Gheysen, G., Kushnir, S., Van Montagu, M., Inze, D., and Castresana, C. (1992). Suppression of β-1,3-glucanase transgene expression in homozygous plants. EMBO J. **11:** 2595–2602.

Dimond, R.L., Farnsworth, P.A., and Loomis, W.F. (1976). Isolation and characterization of mutations affecting UDPG pyrophosphorylase activity in *Dictyostelium discoideum*. Dev. Biol. **50:** 169–181.

Dong, X. (2004). Function Investigation of *Arabidopsis* Callose Synthases and the Signal Transduction Pathway. PhD dissertation (Columbus, OH: Ohio State University).

Dong, X., Hong, Z., Sivaramakrishnan, M., Mahfouz, M., and Verma, D.P. (2005). Callose synthase (CalS5) is required for exine formation during microgametogenesis and for pollen viability in *Arabidopsis*. Plant J. **42:** 315–328.

Dorion, S., Lalonde, S., and Saini, H.S. (1996). Induction of male sterility in wheat by meiotic-stage water deficit is preceded by a decline in invertase activity and changes in carbohydrate metabolism in anthers. Plant Physiol. **111:** 137–145.

Dorlhac de Borne, F., Vincentz, M., Chupeau, Y., and Vaucheret, H. (1994). Co-suppression of nitrate reductase host genes and transgenes in transgenic tobacco plants. Mol. Gen. Genet. **243:** 613–621.

Eimert, K., Villand, P., Kilian, A., and Kleczkowski, L.A. (1996). Cloning and characterization of several cDNAs for UDP-glucose pyrophosphorylase from barley (*Hordeum vulgare*) tissues. Gene **170:** 227–232.

Eschrich, W. (1980). Free space invertase, its possible role in phloem unloading. Ber. Dtsch. Bot. Ges. **93:** 363–378.

Feng, J.H., Lu, Y.G., Liu, X.D., and Xu, X.B. (2001). Pollen development and its stages in rice (*Oryza sativa* L.). Chin. J. Rice Sci. **15:** 21–28.

Flores-Diaz, M., Alape-Giron, A., Persson, B., Pollesello, P., Moos, M., von Eichel-Streiber, C., Thelestam, M., and Florin, I. (1997). Cellular UDP-glucose deficiency caused by a single point mutation in the UDP-glucose pyrophosphorylase gene. J. Biol. Chem. **272:** 23784–23791.

Gemignani, F., Sazani, P., Morcos, P., and Kole, R. (2002). Temperature-dependent splicing of β-globin pre-mRNA. Nucleic Acids Res. **30:** 4592–4598.

Gibeaut, D.M. (2000). Nucleotide sugars and glucosyltransferases for synthesis of cell wall matrix polysaccharides. Plant Physiol. Biochem. **38:** 69–80.

Goetz, M., Godt, D.E., Guivarc'h, A., Kahmann, U., Chriqui, D., and Roitsch, T. (2001). Induction of male sterility in plants by metabolic engineering of the carbohydrate supply. Proc. Natl. Acad. Sci. USA **98:** 6522–6527.

Hamilton, A.J., and Baulcombe, D.C. (1999). A species of small antisense RNA in posttranscriptional gene silencing in plants. Science **286:** 950–952.

Hart, C.M., Fischer, B., Neuhaus, J.M., and Meins, F., Jr. (1992). Regulated inactivation of homologous gene expression in transgenic *Nicotiana sylvestris* plants containing a defense-related tobacco chitinase gene. Mol. Gen. Genet. **235:** 179–188.

Heslop-Harrison, J., and Mackenzie, A. (1967). Autoradiography of soluble [2–14-C]thymidine derivatives during meiosis and microsporogenesis in *Lilium* anthers. J. Cell Sci. **2:** 387–400.

Hiei, Y., Ohta, S., Komari, T., and Kumashiro, T. (1994). Efficient transformation of rice (*Oryza sativa* L.) mediated by *Agrobacterium* and sequence analysis of the boundaries of the T-DNA. Plant J. **6:** 271–282.

Hughes, M., Arundhati, A., Lunness, P., Shaw, P.J., and Doonan, J.H. (1996). A temperature-sensitive splicing mutation in the bimG gene of Aspergillus produces an N-terminal fragment which interferes with type 1 protein phosphatase function. EMBO J. **15:** 4574–4583.

Itoh, J., Nonomura, K., Ikeda, K., Yamaki, S., Inukai, Y., Yamagishi, H., Kitano, H., and Nagato, Y. (2005). Rice plant development: From zygote to spikelet. Plant Cell Physiol. **46:** 23–47.

Johansson, H. (2003). Gene Regulation of UDP-Glucose Synthesis and Metabolism in Plants. PhD dissertation (Umeå, Sweden: Umeå University).

Katsube, T., Kazuta, Y., Mori, H., Nakano, K., Tanizawa, K., and Fukui, T. (1990). UDP-glucose pyrophosphorylase from potato tuber: cDNA cloning and sequencing. J. Biochem. (Tokyo) **108:** 321–326.

Kleczkowski, L.A. (1994). Glucose activation and metabolism through UDP-glucose pyrophosphorylase in plants. Phytochemistry **37:** 1507–1515.

Kleczkowski, L.A., Geisler, M., Ciereszko, I., and Johansson, H. (2004). UDP-glucose pyrophosphorylase. An old protein with new tricks. Plant Physiol. **134:** 912–918.

Koonjul, P.K., Minhas, J.S., Nunes, C., Sheoran, I.S., and Saini, H.S. (2005). Selective transcriptional down-regulation of anther invertases precedes the failure of pollen development in water-stressed wheat. J. Exp. Bot. **56:** 179–190.

Kurata, N., Miyoshi, K., Nonomura, K., Yamazaki, Y., and Ito, Y. (2005). Rice mutants and genes related to organ development, morphogenesis and physiological traits. Plant Cell Physiol. **46:** 48–62.

Lechtenberg, B., Schubert, D., Forsbach, A., Gils, M., and Schmidt, R. (2003). Neither inverted repeat T-DNA configurations nor arrangements of tandemly repeated transgenes are sufficient to trigger transgene silencing. Plant J. **34:** 507–517.

Lindbo, J.A., Silva-Rosales, L., Proebsting, W.M., and Dougherty, W.G. (1993). Induction of a highly specific antiviral state in transgenic plants: Implications for regulation of gene expression and virus resistance. Plant Cell **5:** 1749–1759.

Mamun, E.A., Alfred, S., Cantrill, L.C., Overall, R.L., and Sutton, B.G. (2006). Effects of chilling on male gametophyte development in rice. Cell Biol. Int. **30:** 583–591.

Mu, H. (2002). Screening of Genes Related to Pollen Development in a Thermo-Sensitive Male Sterile Rice (*Oryza sativa* L.): Cloning and Characterization of UDP-Glucose Pyrophosphorylase. PhD dissertation (Hong Kong, China: University of Hong Kong).

Napoli, C., Lemieux, C., and Jorgensen, R. (1990). Introduction of a chimeric chalcone synthase gene into petunia results in reversible cosuppression of homologous genes in trans. Plant Cell **2:** 279–289.

Oliver, S.N., Van Dongen, J.T., Alfred, S.C., Mamun, E.A., Zhao, X.C., Saini, H.S., Fernandes, S.F., Blanchard, C.L., Sutton, B.G., Geigenberger, P., Dennis, E.S., and Dolferus, R. (2005). Cold-induced repression of the rice anther-specific cell wall invertase gene OSINV4 is correlated with sucrose accumulation and pollen sterility. Plant Cell Environ. **28:** 1534–1551.

Owen, H.A., and Makaroff, C.A. (1995). Ultrastructure of microsporogenesis and microgametogenesis in *Arabidopsis thaliana* (L.) Heynh. ecotype Wassilewskija (Brassicaceae). Protoplasma **185:** 7–21.

Polowick, P.L., and Sawhney, V.K. (1992). Ultrastructural changes in the cell wall, nucleus and cytoplasm of pollen mother cells during meiotic prophase I in *Lycopersicon esculentum* (Mill.). Protoplasma **169:** 139–147.

Que, Q., Wang, H.Y., English, J.J., and Jorgensen, R.A. (1997). The frequency and degree of cosuppression by sense chalcone synthase

transgenes are dependent on transgene promoter strength and are reduced by premature nonsense codons in the transgene coding sequence. Plant Cell **9:** 1357–1368.

Ranwala, A.P., and Miller, W.B. (1998). Sucrose-cleaving enzymes and carbohydrate pools in *Lilium longiflorum* floral organs. Physiol. Plant **103:** 541–550.

Sablowski, R.W., and Meyerowitz, E.M. (1998). Temperature-sensitive splicing in the floral homeotic mutant apetala3-1. Plant Cell **10:** 1453–1463.

Sambrook, J., Fritsch, E.F., and Maniatis, T. (1989). Molecular Cloning: A Laboratory Manual, 2nd ed. (Cold Spring Harbor, NY: Cold Spring Harbor Laboratory Press).

Sheoran, I.S., and Saini, H.S. (1996). Drought-induced male sterility in rice: Changes in carbohydrate levels and enzyme activities associated with the inhibition of starch accumulation in pollen. Sex. Plant Reprod. **9:** 161–169.

Sowokinos, J.R., Spychalla, J.P., and Desborough, S.L. (1993). Pyrophosphorylases in *Solanum tuberosum* (IV. Purification, tissue localization, and physicochemical properties of UDP-glucose pyrophosphorylase). Plant Physiol. **101:** 1073–1080.

Spychalla, J.P., Scheffler, B.E., Sowokinos, J.R., and Bevan, M.W. (1994). Cloning, antisense RNA inhibition and the coordinated expression of UDP-glucose pyrophosphorylase with starch biosynthetic genes in potato tubers. J. Plant Physiol. **144:** 444–453.

Szittya, G., Silhavy, D., Molnar, A., Havelda, Z., Lovas, A., Lakatos, L., Banfalvi, Z., and Burgyan, J. (2003). Low temperature inhibits RNA silencing-mediated defence by the control of siRNA generation. EMBO J. **22:** 633–640.

Truernit, E., Stadler, R., Baier, K., and Sauer, N. (1999). A male gametophyte-specific monosaccharide transporter in *Arabidopsis*. Plant J. **17:** 191–201.

Tucker, M.R., Paech, N.A., Willemse, M.T., and Koltunow, A.M. (2001). Dynamics of callose deposition and β-1,3-glucanase expression during reproductive events in sexual and apomictic *Hieracium*. Planta **212:** 487–498.

Valla, S., Coucheron, D.H., Fjaervik, E., Kjosbakken, J., Weinhouse, H., Ross, P., Amikam, D., and Benziman, M. (1989). Cloning of a gene involved in cellulose biosynthesis in *Acetobacter xylinum*: Complementation of cellulose-negative mutants by the UDPG pyrophosphorylase structural gene. Mol. Gen. Genet. **217:** 26–30.

van der Krol, A.R., Mur, L.A., Beld, M., Mol, J.N., and Stuitje, A.R. (1990). Flavonoid genes in petunia: Addition of a limited number of gene copies may lead to a suppression of gene expression. Plant Cell **2:** 291–299.

Vaucheret, H., Nussaume, L., Palauqui, J.C., Quillere, I., and Elmayan, T. (1997). A transcriptionally active state is required for post-transcriptional silencing (cosuppression) of nitrate reductase host genes and transgenes. Plant Cell **9:** 1495–1504.

Virmani, S.S., Sun, Z.X., Mou, T.M., Ali, A.J., and Mao, C.X. (2003). Two-Line Hybrid Rice Breeding Manual. (Los Baños, Philippines: International Rice Research Institute).

Waterkeyn, L. (1962). Les parois microsporocytaires de nature callosique chez Helleborus et Fadescantia. Cellule **62:** 225–255.

Waterkeyn, L., and Beinfait, A. (1970). On a possible function of the callosic special wall in *Ipomoea purpurea* (L.) Roth. Grana **10:** 13–20.

Weidenhammer, E.M., Singh, M., Ruiz-Noriega, M., and Woolford, J.L., Jr. (1996). The PRP31 gene encodes a novel protein required for pre-mRNA splicing in *Saccharomyces cerevisiae*. Nucleic Acids Res. **24:** 1164–1170.

Wesley, S.V., et al. (2001). Construct design for efficient, effective and high-throughput gene silencing in plants. Plant J. **27:** 581–590.

Winter, H., and Huber, S.C. (2000). Regulation of sucrose metabolism in higher plants: Localization and regulation of activity of key enzymes. Crit. Rev. Biochem. Mol. Biol. **35:** 253–289.

Worrall, D., Hird, D.L., Hodge, R., Paul, W., Draper, J., and Scott, R. (1992). Premature dissolution of the microsporocyte callose wall causes male sterility in transgenic tobacco. Plant Cell **4:** 759–771.

Ylstra, B., Garrido, D., Busscher, J., and van Tunen, A.J. (1998). Hexose transport in growing petunia pollen tubes and characterization of a pollen-specific, putative monosaccharide transporter. Plant Physiol. **118:** 297–304.

Yost, H.J., and Lindquist, S. (1986). RNA splicing is interrupted by heat shock and is rescued by heat shock protein synthesis. Cell **45:** 185–193.

Yost, H.J., and Lindquist, S. (1991). Heat shock proteins affect RNA processing during the heat shock response of *Saccharomyces cerevisiae*. Mol. Cell. Biol. **11:** 1062–1068.

Zrenner, R., Willmitzer, L., and Sonnewald, U. (1993). Analysis of the expression of potato uridinediphosphate-glucose pyrophosphorylase and its inhibition by antisense RNA. Planta **190:** 247–252.